Improved Tunability And Energy Storage Density Properties Of Low Loss, Lead Free (Ba0.50Sr0.50)Tio3 And Ba(Zr0.15Ti0.85)O3 Bilayer Thin Film Stacks

M.L.V. Mahesh (mahesh.mlv@gmail.com)
DMRL: DRDO Defence Metallurgical Research Laboratory https://orcid.org/0000-0002-9274-5522
Prem Pal
IITH: Indian Institute of Technology Hyderabad
Bhanu Prasad V.V.
DMRL: DRDO Defence Metallurgical Research Laboratory
A.R. James
DMRL: DRDO Defence Metallurgical Research Laboratory

Original Research

Keywords: MgO, SrTiO3, BST, BZT, FoM

Posted Date: February 10th, 2021

DOI: https://doi.org/10.21203/rs.3.rs-202913/v1

Version of Record: A version of this preprint was published at Journal of Electronic Materials on November 24th, 2021. See the published version at https://doi.org/10.1007/s11664-021-09329-1.

Declarations

Funding

No funding was received.

Conflicts of interest/Competing interests

The authors declare that they have no known competing financial interests or personal relationships that could have appeared to influence the work reported in this paper.

Availability of data and material

It is hereby declared that the material is exclusively prepared in Defence Metallurgical research laboratory, Hyderabad, INDIA and the data and material is available with the authors.

Code availability

Not applicable.

Authors' contributions

All authors contributed equally to the manuscript.

IMPROVED TUNABILITY AND ENERGY STORAGE DENSITY PROPERTIES OF LOW LOSS, LEAD FREE $(Ba_{0.50}Sr_{0.50})TiO_3$ and $Ba(Zr_{0.15}Ti_{0.85})O_3$ BILAYER THIN FILM STACKS

M.L.V. Mahesh[*,1,2], Prem Pal[2], V.V.Bhanu Prasad[1], & A.R. James[1]

1) *Ceramics & Composites Group, Defence Metallurgical Research Laboratory, Kanchanbagh, Hyderabad-500058*
2) *Department of Physics, Indian Institute of Technology, Sangareddy, Kandi, Telangana 502285*

**email : mahesh@dmrl.drdo.in*

Abstract

Multilayer thin films of $(Ba_{0.50}Sr_{0.50})TiO_3$ (BST) and $Ba(Zr_{0.15}Ti_{0.85})O_3$ (BZT) were designed and grown using Pulsed LASER Deposition technology. The periodic $(BST/BZT)_n$ thin films were deposited on Pt‹111›/SiO_2/Si substrates. X-ray diffraction reveals the presence of a polycrystalline, perovskite structure corresponding to the bilayer thin film stacks. SEM analysis confirmed the multilayer structure without any interdiffusion across layers. It was also found that the dielectric and ferroelectric properties of the thin films are strongly influenced by the periodic hetero-structures. The thin film stacks exhibit significantly higher tunabilities, comparable with multilayer thin films grown on various single crystal substrates such as $LaAlO_3$, MgO and $SrTiO_3$. Possible mechanisms explaining the other observed attributes such as lower dielectric loss resulting in higher Figure of Merit (FoM), low leakage current are discussed. The effect of incorporating a comparatively lower permittivity thin film in the multilayer stacks is presented. The observed properties of

such multilayer structured films help in realization of low loss and highly tunable applications.

*Corresponding author Tel. : +91 40 24586885, FAX: +91 40 2434 0681

E-mail address :mahesh@dmrl.drdo.in, mahesh.mlv@gmail.com

1. Introduction

Dielectric capacitors play an important role in the development of electric industry due to their high power density (up to 100W/kg), faster charge-discharge capabilities, longer life time, temperature stable electrical properties especially in advanced electronics and electrical power systems such as hybrid electric vehicles, high frequency inverters, and power grids [1-2]. However, the achieved energy storage density of the dielectric capacitors is much lower than their electrochemical counterparts, such as Li-ion batteries and double layer supercapacitors. Researchers are trying to improve the energy storage density of dielectric capacitors coupled with minimum dielectric loss over the past decades.

Tunable devices exhibit decrease in capacitance with increasing applied electric field and thus find numerous applications viz., tunable filters, phase shifters, voltage controlled oscillators. $(Ba_{1-x}Sr_x)TiO_3$ is an extensively studied material system for numerous high frequency applications [3]. Several studies were reported with domain engineering, doping, modification of stress and strain in the films, growing films of different Ba/Sr & (Ba+Sr)/Ti ratios to improve the film material properties [4]. Energy storage devices at different working temperatures can be fabricated using these materials owing to the material's property to attain high dielectric constant at desired temperatures by controlling composition of the

constituents. However, the relatively low breakdown strength as well as poor temperature stability near T_C limits its application in dielectric capacitors [5].

Growing multilayered dielectric/ferroelectric thin films and superlattices is an effective way to improve properties of dielectric/ferroelectric thin films. A multilayer approach, in which the film is composed of alternating layers of different compositions or even different materials, appears to be very promising in optimizing the properties of materials. Pulsed laser deposition (PLD) is the most preferred method for deposition of ferroelectric multilayered thin films and superlattices to maintain stoichiometry. Bilayer thin film structures consisting of one layer as BST (a paraelectric composition) and another layer of $(Ba_{1-x}Sr_x)TiO_3$ with composition gradient [6-8], multiferroic [9], ferroelectric [10-11], non-ferroelectric [12-13], conducting perovskite [12,14-15], doped multilayers of BST thin films [16] have been reported. Another interesting sandwich structure of ferroelectric thin films gained much attention due to improved electrical properties [10,17-20]. Zhao et. al. studied stress at interfaces in a trilayered structure [21]. Multilayer structures resulted in better dielectric properties, decreased loss tangents, enhanced tunabilitites, improved fatigue resistant properties [9,22-23]. Organic-inorganic (Ferroelectric - poly vinylidene fluoride) composites displayed low dielectric constant (~30) and were not resistant to high temperature [24].

Reports on BST with another layer of material near morphotropic phase boundary (MPB) are not reported in the literature. Compositions near MPB exhibit superior properties due to contribution of all polar vectors of various coexisting phases. Hence, Barium zirconium titanate $Ba(Zr_{0.15}Ti_{0.85})O_3$ (BZT) is chosen as another layer in this bilayer pattern of the multilayer structure. BZT material system exhibits several interesting features among the dielectric behaviour of doped $BaTiO_3$

materials. BZT has attracted immense attention because of its potential applications in the microwave technology, due to improved chemical stability, low dielectric loss and large tunability [25]. The substitution of Zr^{4+} for Ti^{4+} reduces average grain size and maintains the leakage current low and stable. In this report, the electric properties of the multilayer structure of $(Ba_{0.50}Sr_{0.50})TiO_3$ and $Ba(Zr_{0.15}Ti_{0.85})O_3$ thin films are studied.

The motivation of this article is to develop and characterize a multilayer $(BST/BZT)_n$ thin film structure which can exhibit high tunability coupled with low loss due to incorporation of Zr in the lattice. The highly tunable, low loss and medium permittivity multilayer thin film structure is designed and grown successfully. We expect to improve the efficiency of energy storage performance of multilayer structure by combining the high permittivity of BST material system and the low loss, high breakdown characteristics of BZT materials.

2. Experimental procedure

A multilayer structure consisting of bi-layers of $(Ba_{0.50}Sr_{0.50})TiO_3$ (BST) and $Ba(Zr_{0.15}Ti_{0.85})O_3$ (BZT) was designed as shown in Fig. 1 and realized with the help of pulsed laser deposition (PLD) technique using two individual BZT and BST targets of 1-inch diameter. Preparation of targets was carried out by adopting solid state reaction method using a high-energy planetary ball mill. Full details of the preparation of targets [26] and film growth [27-28] were reported in our previous study.

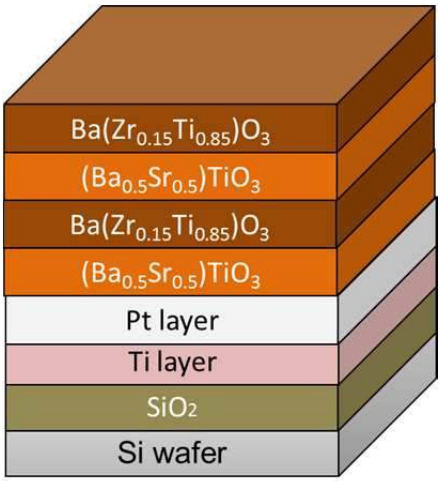

Fig. 1 Schematic of multilayer structure consisting of bilayer stack of $(Ba_{0.50}Sr_{0.50})TiO_3$ and $Ba(Zr_{0.15}Ti_{0.85})O_3$ thin films

An X-ray diffractometer (Philips X'Pert PW-3020) with a monochromatic Cu-K_α radiation (λ= 1.542Å) was used over a 2θ range from 20^o to 60^o to characterize the crystalline phase of the $(BST/BZT)_n$ bilayers stack. Gold electrodes of 400 μm diameter are deposited on the multilayers by a table top sputtering system (Denton Vacuum Desk IV) using a grid mask for carrying out electrical characterization. The polarization versus electric field (P–E) hysteresis loops, leakage current characteristics and voltage dependent capacitance curves of the multilayer thin films were recorded using a ferroelectric test system (M/s. aixAcct Systems, GmbH, Germany) which works in the virtual ground mode using a triangular waveform, at room temperature.

3. Results and discussion

3.1 Crystal structure

Fig. 2 shows the room temperature X-ray diffractograms (XRD) of multilayer structure comprising of $(BST/BZT)_n$ bi-layers with n=2. The multilayer thin films

exhibit pure perovskite phase and no secondary phase is observed in the entire range of investigation. The characteristic single phase, randomly oriented polycrystalline growth can be observed from Fig. 2. The presence of both BST as well as BZT phases can be noticed from the X-ray diffractograms. The phase purity crystalline nature confirmed from the measured intensities and the values of the full-width-half maximum (FWHM) of the diffraction peaks. We could not detect any reflection corresponding to any impurity phase in the XRD spectra, suggesting impurity free single phase growth of the multilayer thin films. The diffraction pattern also confirms that there was no measurable reaction between BST and BZT multilayers.

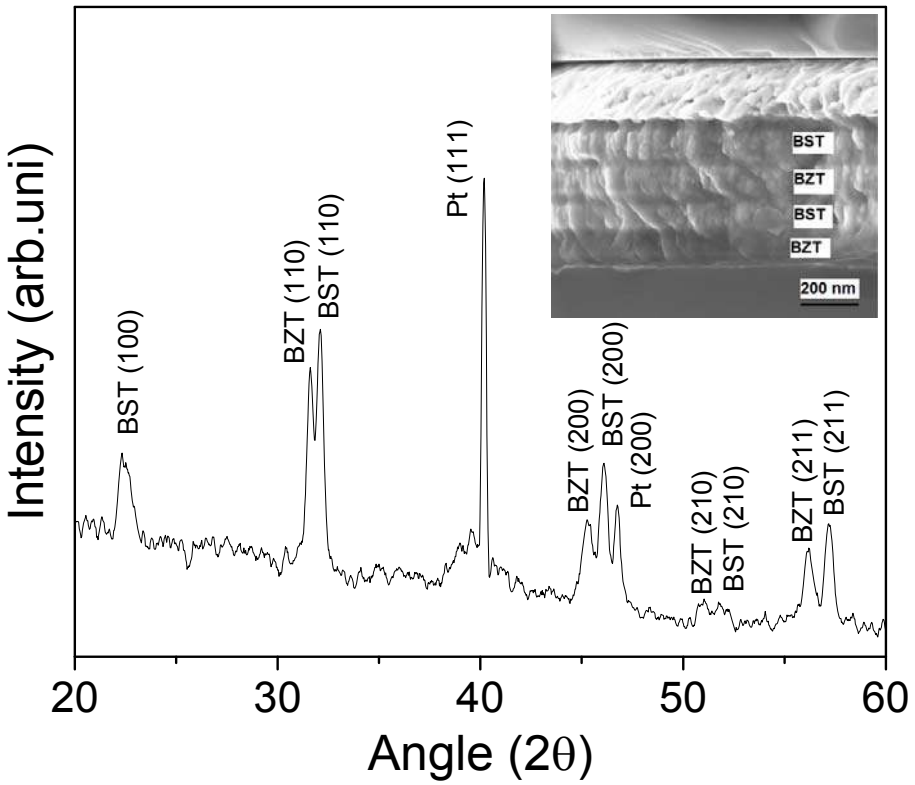

Fig. 2 X-ray diffractograms of $(Ba_{0.50}Sr_{0.50})TiO_3$ and $Ba(Zr_{0.15}Ti_{0.85})O_3$ multilayer thin films (inset) Cross section SEM images depicting multilayer structure.

The cross section SEM images of multi layered $(BST/BZT)_n$ stack with n=2 is shown in the inset of Fig.2. The total thickness of the multilayer structure as found from SEM, matches with the surface profiler results. It is also observed from Fig.2 that the peaks corresponding to {110}, {200}, {211} reflections of multilayer thin film of BST and BZT are in the near vicinity of each other indicating similar structure and also highlights absence of diffusion of dopant ions across individual layers. Lattice parameters of Pt, BST and BZT layers are found to be 3.925 A^o, 3.97 A^o, and 4.02 A^o, respectively. A gradual increase in the unit cell lattice parameters assisted in relieving the lattice strain generated near the interfaces. The lattice parameters of BST thin films are close those reported for $(Ba_{0.50}Sr_{0.50})TiO_3$ films [10,12], which indicate the cubic ABO_3 perovskite structure of grown thin films.

3.2 Dielectric properties

The electric field dependent dielectric constant and dielectric loss characteristics measured at 1MHz at room temperature corresponding to the multi-layer structure of $(BST/BZT)_n$ with n=2 fabricated by PLD technique are shown in Fig.3. The contribution of dielectric constant corresponding to BST/BZT multi-layer structure is not only due to the contribution as predicted by Maxwell–Wagner model [6], but also from other contributions such as strain induced polarization, mismatch of lattice parameters of individual layers [29-30] and the contribution of co-existent phases present in the morphotropic phase boundary composition corresponding to BZT thin films [25].

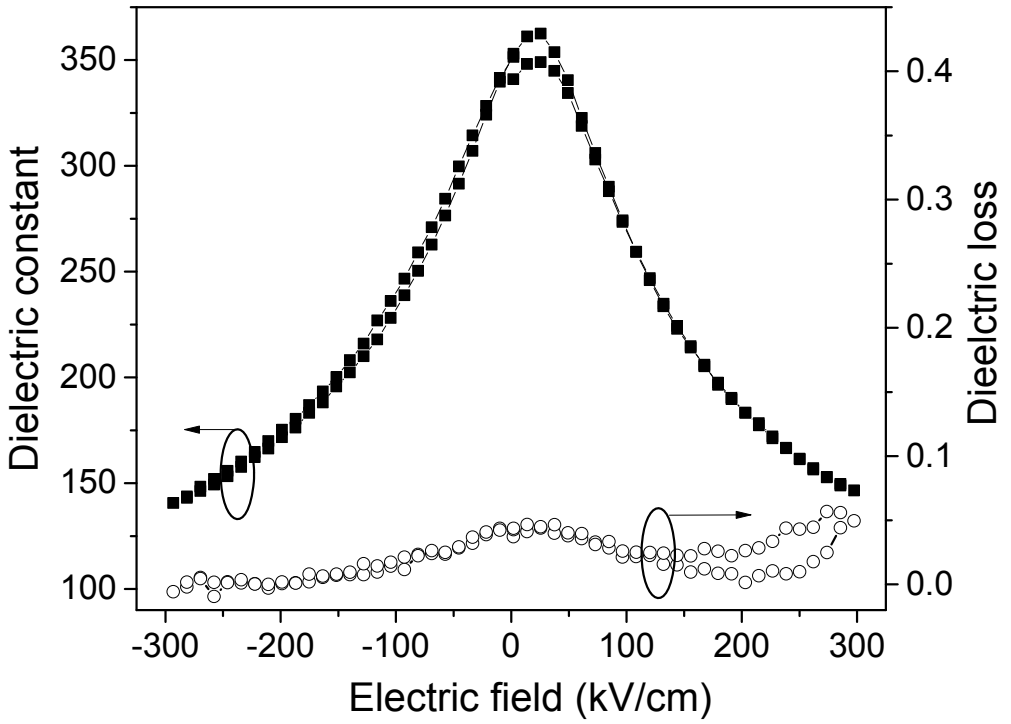

Fig. 3 Electric field dependence of dielectric permittivity and dielectric loss corresponding to bilayers of $(Ba_{0.50}Sr_{0.50})TiO_3$ and $Ba(Zr_{0.15}Ti_{0.85})O_3$ multilayer thin films at room temperature.

The effective capacitance of a multilayer structure can be obtained by considering the capacitances of all constituent thin films. Hence, the effective capacitance, C_{eff}, can be explained by the series combination of BST and BZT films and can be calculated by the formula:

$$\frac{1}{C_{eff}} = \left(\frac{1}{C_{BST}} + \frac{1}{C_{BZT}}\right) + \ldots\ldots + \left(\frac{1}{C_{BST}} + \frac{1}{C_{BZT}}\right) = n\left(\frac{1}{C_{BST}} + \frac{1}{C_{BZT}}\right) \qquad (1)$$

Where n, C_{BST} and C_{BZT} represents number of (BST/BZT) multi layers, capacitance of BST thin films and capacitance of BZT thin films, respectively. The effective dielectric constant, ε_{eff} of multi-layer structure consisting of n bilayers of BST & BZT can be obtained from Eq (1) as :

$$\frac{n(t_{BST}+t_{BZT})}{\varepsilon_{eff}} = n\left(\frac{t_{BST}}{\varepsilon_{BST}} + \frac{t_{BZT}}{\varepsilon_{BZT}}\right) \quad (2)$$

Where t_{BST} and t_{BZT} are thicknesses of the BST and BZT thin films, respectively. In this study the thickness of BST and BZT thin films is kept constant. Therefore from Eq. (2)

$$\varepsilon_{eff} = 2\left(\frac{\varepsilon_{BST}\times\varepsilon_{BZT}}{\varepsilon_{BST}+\varepsilon_{BZT}}\right) = \left(\frac{2}{1+\frac{\varepsilon_{BZT}}{\varepsilon_{BST}}}\right)\varepsilon_{BZT} \quad (3)$$

The dielectric constant of BST thin films is greater than dielectric constant of BZT thin films, $\varepsilon_{BST}>\varepsilon_{BZT}$ [31]. Using $(\varepsilon_{BZT}/\varepsilon_{BST})<1$ in eq (3) demonstrates that the effective dielectric constant, ε_{eff} lies between the dielectric constant of individual multi layers BST and BZT thin films i.e., $\varepsilon_{BST}>\varepsilon_{eff}>\varepsilon_{BZT}$. Similar results were reported for compositionally graded multilayer thin films [6]. The electric field dependence of dielectric constant of the bilayer structure shown in Fig. 3 highlights the paraelectric nature of the stacked $(BST/BZT)_n$ thin films. In addition, dielectric loss (tanδ) is also an important factor for capacitors. The dielectric loss of multilayer is found to be <0.05 throughout the measured range of applied electric fields i.e., from -300 kV/cm to 300 kV/cm. The uniform low dielectric loss is another notable feature of the stacked structure of thin films. However, at relatively higher fields (>200 kV/cm) non-uniform dielectric loss with respect to the direction of applied fields can be due to parasitic capacitance, unusual charge accumulation near the top BZT layer and electrode interface.

The improved dielectric loss is due to defect trapping at interfaces or immobilization of defects to compensate polarization difference between thin film layers [7], incorporation of chemically stable Zr^{+4} ion in BZT thin film and also due to minimised lattice mismatch between different layers of fabricated structure such as

BST and the Pt (111) substrate, BZT and BST thin films. Several challenges involved in the process optimization such as obtaining a sharp interface between different layers, uniform growth of thin films, sequential and periodic and repetitive selection of target materials etc. were addressed, thereby realizing uniform multi-layered stack. All of these require careful optimization of PLD deposition parameters like LASER energy fluence, repetition rate, target-substrate distance, oxygen partial pressure, deposition temperature, thickness control etc. Each of these process parameters was carefully taken cognizance of in this research. The uniform layer thicknesses in the stack lead to consistent electrical properties across the sample.

3.3 Tunability Studies

The ability of a material to change its capacitance with increase in applied voltage is termed as tunability and is determined by the ratio of change in capacitance on application of applied voltage to the capacitance at zero bias voltage i.e., $(C_0-C_V)/C_0$ where C_0 and C_V are capacitance at zero voltage and applied voltage, respectively. Tunability is an essential parameter in understanding the behaviour of a material at high voltages. The capacitance vs. electric field loops corresponding to $(BST/BZT)_n$ thin films are shown in Fig. 4. The zero-field capacitance at 1 MHz is found to be >1.3 nF and is found to decrease with rise in applied field. Such high capacitance values are ascribed to inhomogeneous dielectric structure and resistivity of the bilayer thin film stack. The tunability of multilayer thin films is found to be 70% at an applied bias voltage of 12V and there was also no evidence of saturation in tunability up to the maximum measured bias voltage. Therefore, higher tunability can be expected by further increasing the bias voltage. The observed tunability values are better than epitaxial films of lead free

materials of $(Ba_{1-x}Sr_x)TiO_3$ and / or $Ba(Zr_{1-y}Ti_y)O_3$ multilayer structures grown on single crystal substrates viz., $LaAlO_3$ [15], MgO [32] and $SrTiO_3$ [33] and other polycrystalline heterostructure multilayer thin films [6, 8, 10-14, 17-20, 34].

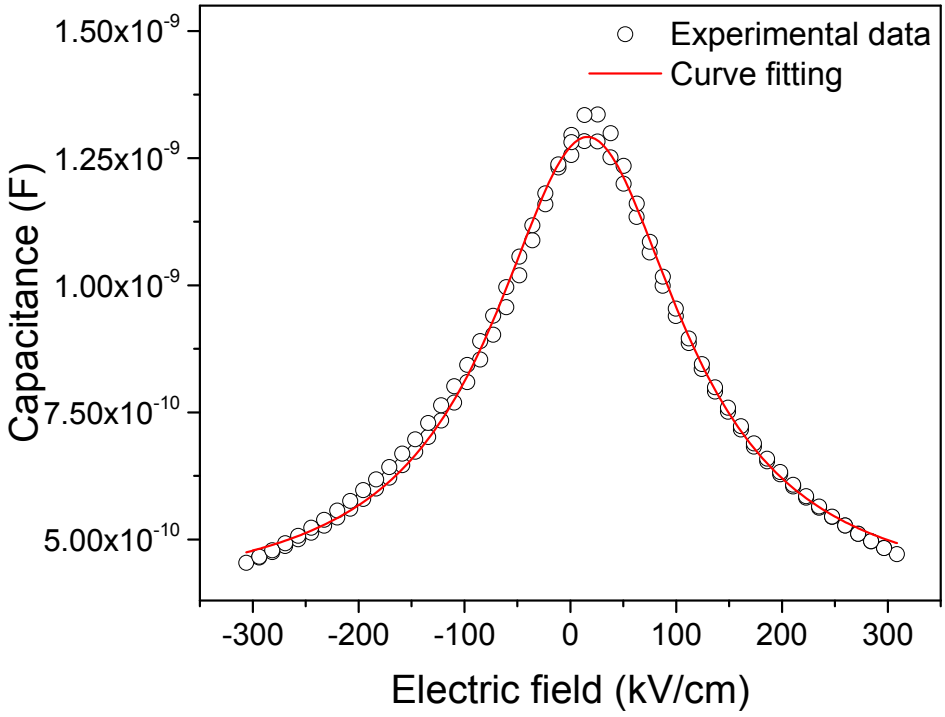

Fig. 4 Capacitance as a function of electric field corresponding to bilayers of $(Ba_{0.50}Sr_{0.50})TiO_3$ and $Ba(Zr_{0.15}Ti_{0.85})O_3$ multilayer thin films.

The ability to withstand high voltages without breaking down indicates the appearance of dielectric enhancement in multilayer heterogeneous structures. The enhancement can be explained by considering the Maxwell-Wagner series capacitor model [6] and ascribed to stress between different layers caused by lattice mismatch, which is often discussed in super-lattice structures [35]. Layered structures have a strong influence on the electric field distribution. The relationship between field distribution and permittivity in a layered composite system [36]

consisting of different layers say A and B possessing different permittivities, ε_A, ε_B and thicknesses, d_A and d_B respectively can be expressed as :

$$E_A = \frac{\varepsilon_B d}{\varepsilon_A d_B + \varepsilon_B d_A} E \quad (4)$$

$$E_B = \frac{\varepsilon_A d}{\varepsilon_A d_B + \varepsilon_B d_A} E \quad (5)$$

where d = (d_A + d_B) is the total thickness of the multilayer structure, E_A and E_B are theoretical electric fields of layers A and B, respectively. It can be noticed from Eq (4) and (5) that the dielectric layers with lower permittivity (BZT thin films in this case) will experience higher electric fields than the applied field. The higher electric field assists in obtaining enhanced tunability. Hence, BZT thin film's contribution in the multilayer structure studied is responsible in obtaining low loss and improved tunability. The space charge accumulates at the interface between BST and BZT layers, forming low resistance interfacial regions [37] resulting in enhanced properties.

The C-V loops recorded at room temperature illustrates that the multilayer stack of BST/BZT thin films is in the paraelectric state with a weak hysteresis behaviour. Johnson reported phenomenological theory [38] explaining the explicit relationship between the dielectric constant and the applied electric field as below :

$$\varepsilon_{r(E)} = \frac{\varepsilon_{r(0)}}{\left[1+\alpha \varepsilon_{r(0)}{}^3 E^2\right]^{1/3}} \quad (6)$$

where $\varepsilon_{r(0)}$ and $\varepsilon_{r(E)}$ are the dielectric constants at zero electric field and applied electric field E, respectively, and α is the temperature-dependent constant, which provides information on the degree of anharmonic contributions of the polarization to the free energy [39] . As shown in Fig. 4, the experimental data is fitted using Eq. 6. It can be noticed that multilayer films exhibit paraelectric state, and the ε Vs. E

characteristics can be fitted exactly over the whole electric field range from zero to the maximum applied positive voltage and back to zero (positive cycle) and similarly in the negative cycle from zero to the maximum negative voltage. The deviation of the experimental data from the fitting curve is found to be less than 1%. The agreement between the experimental data and the fitting lines of BST/BZT multilayer structure is quite good indicating the self-consistency of that model.

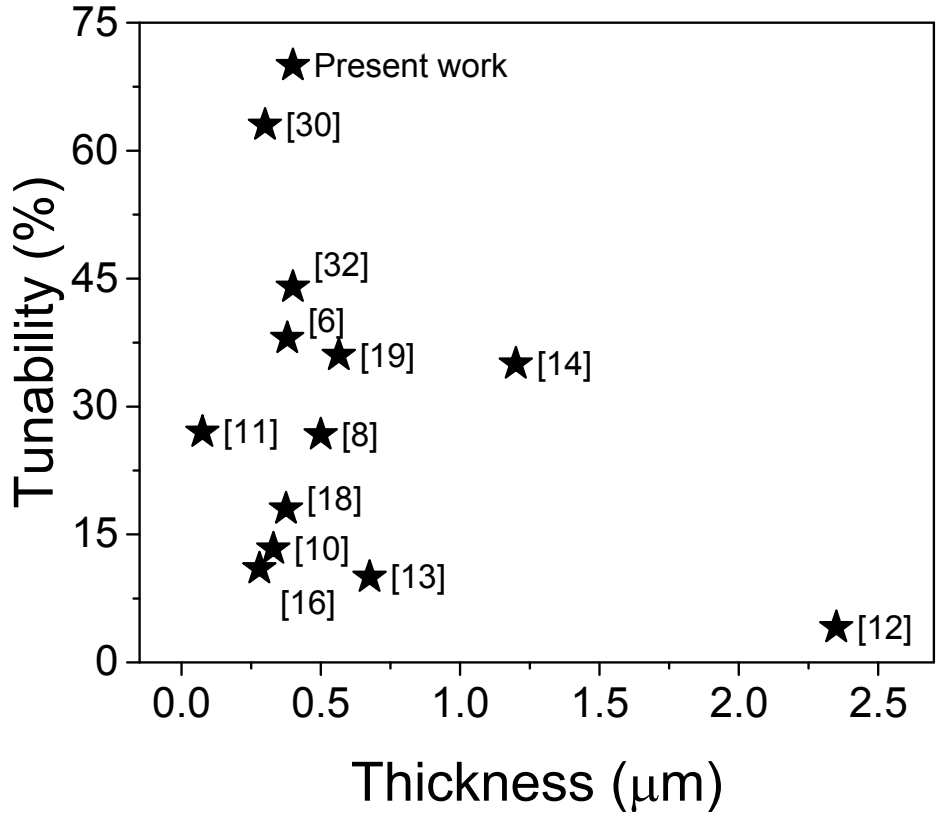

Fig. 5 Reported tunabilities of different lead-free multilayer thin films vs total thickness of the grown multilayers using different processing techniques and substrates.

The tunability values for multilayer thin films grown on different substrates using different methods are compiled and shown in Fig. 5. It can be noticed that the obtained tunability values of $(BST/BZT)_n$ bilayer stack of multilayer thin films is higher

than reported values of various multilayer thin films including the heterostructure thin films grown on single crystal substrates [15,32-33]. Gradual change in lattice parameters of bilayer thin films stack, composition near MPB, low dielectric loss resulted due to incorporation of BZT layer are considered as contributory factors to the observed enhanced tunabilities.

3.4 Field dependent Polarization curves

The room temperature polarization-electric field (P-E) curves of BST/BZT multilayer thin film structure measured at 100 kHz frequency is shown in Fig. 6. The onset of saturation in polarization at high fields can be observed from P-E loops of bilayer film stacks consisting of a paraelectric layer. The multilayer structure influences not only on the ionic polarization but also the electronic structure or chemical bonding nature of the bilayer stack of BST/BZT thin films. The results suggest that the multilayer thin films exhibit linear dependence on applied voltage to a considerable range. Ferroelectric kind of saturation can be noticed from Fig. 6 at high electric fields measured at room temperature. Such behaviour is attributed to B-site cation movements contributed by different phases of polar vectors that are present at MPB composition in BZT thin films, due to the interfacial coupling of electrostatic and elastic interactions [22].

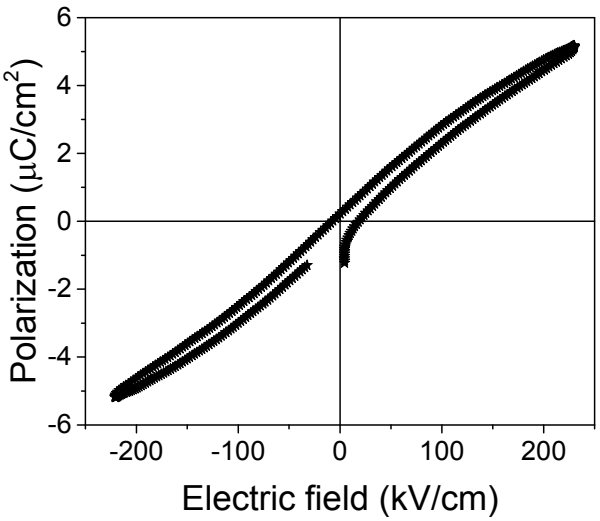

Fig. 6 Evolution of ferroelectric hysteresis loops with respect to the electric field corresponding to lead-free multilayer thin films

3.5 Energy storage properties

The maximum polarization (P_{max}) of $(BST/BZT)_n$ multilayer thin films show strong dependence on the order of layers. The P-E loops illustrate the improved energy storage density (ESD) properties of multilayer structures. As shown in the Fig. 7, the area enclosed by the discharge curve with respect to the polarization axis represents the recoverable energy density, $U_{rec.}$ and the area enclosed between the charge and discharge curves represent energy loss, U_{loss} are shown in Fig.7. It is obvious that high P_{max} and narrow P-E loops will be favourable for energy storage. Generally, the value of energy storage density, U_C can be calculated from P-E loops using the following equation:

$$U_C = \int_0^{E_{max}} E\, dD \cong \int_0^{E_{max}} P\, dE \qquad (7)$$

Where E_{max} is the maximum applied field. It is also found that with increase in number of bilayer stacks maximum polarization also increases and thus result in

improved ESD properties of the multilayer thin films structure. The calculated energy storage density of the multilayer thin films stack is found to be ~0.65 J/cm^3 at relatively low electric field of 225 kV/cm. As expected, the $(BST/BZT)_n$ multilayer films show high breakdown strength and moderate maximum polarization, which is favourable for high energy storage density.

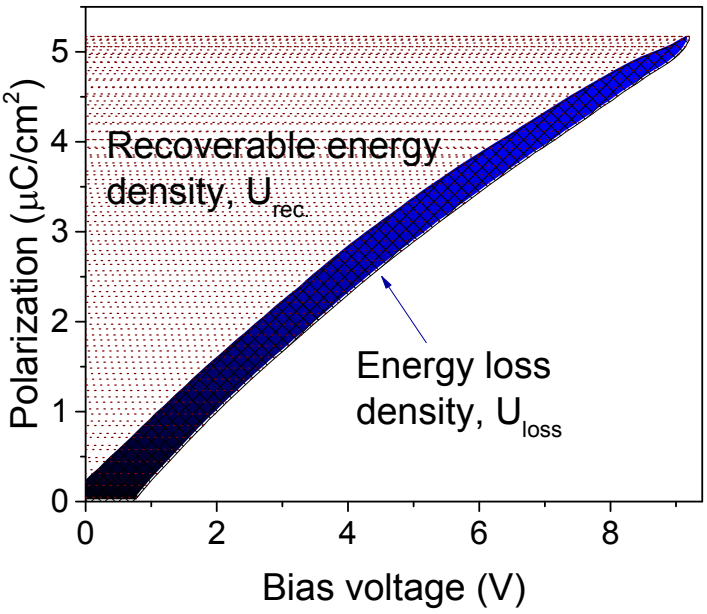

Fig. 7 Polarization vs bias voltage loops highlighting the recoverable energy density, U_{rec} and energy loss, U_{loss}

In actual applications, energy storage efficiency (η) is another very important parameter which can be defined as the ratio of the recoverable energy density, $U_{rec.}$ and the total energy density, U as follows :

$$\eta = \frac{U_{rec.}}{U_{rec.} + U_{loss}} \quad (8)$$

The energy storage efficiencies obtained in this study (~82% at an electric field of 225 kV/cm) is higher than the reported values [40]. Absence of saturation in P-E loops indicates that enhanced energy storage density values can be realized with

further rise in electric field. Improved efficiency, electrical break down strength and dielectric loss were reported with increase in number of multilayers [33,41]. The heterostructure multilayer thin films of BST/BZT bilayer stack resulted in improved efficiency and low dielectric loss by restricting flow of leakage current.

The propagation of electric trees is shown in Fig. 8 when the multilayer thin film stack is subjected to high voltages. At such high voltages, the leakage current path propagates and thus leads to electric breakdown of the film. In this study the bilayers of $(BST/BZT)_n$ thin films are repeated so as to obtain low loss and also to terminate the current carrying path by BZT layers. With the same total thickness, the breakdown electric field, E_B and Energy storage density of the multilayers can be significantly improved by increasing the number of interfaces [41].

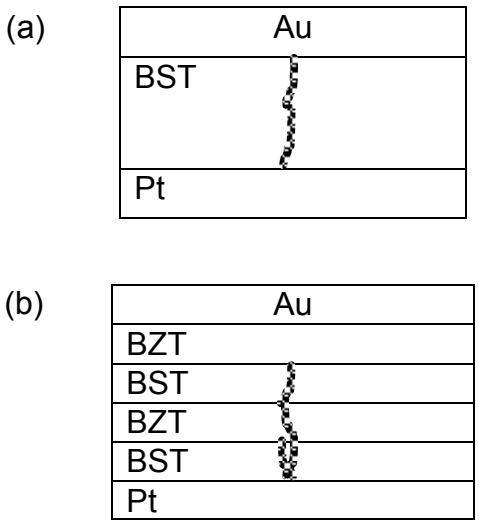

Fig. 8 Schematic illustrating propagation of leakage current conducting path in (a) $(Ba_{0.50}Sr_{0.50})TiO_3$ thin film and (b) Multilayer thin films of $(Ba_{0.50}Sr_{0.50})TiO_3$ and $Ba(Zr_{0.15}Ti_{0.85})O_3$ bilayers.

From Fig. 8 (a) it can be noticed that the leakage current propagates due to the absence of layers that terminate the conduction path whereas in Fig. 8 (b) the BZT layers exhibit an obstruction behaviour at the interfaces to the electrical trees. It is reported that BST thin film layers creates low oxygen vacancy concentration and high energy barrier for oxygen vacancies [9] both of which are known to deteriorate the films properties. In this study, the deposited multilayer thin films are subjected to post annealing in an oxygen rich atmosphere. In-situ oxygen annealing of grown multilayer thin films are also believed to reduce the oxygen vacancy concentration [28]. Morphotropic phase boundary composition of BZT thin films combined with paraelectric BST thin films resulted in enhanced tunability for realization of tunable applications.

5. Conclusions

The effects of bilayer stack of $(Ba_{0.50}Sr_{0.50})TiO_3$ (BST) and $Ba(Zr_{0.15}Ti_{0.85})O_3$ (BZT) thin films deposited on Pt‹111›/SiO_2/Si‹100› substrates using pulsed laser deposition technology on dielectric properties and energy storage behaviour have been investigated. X-ray diffraction reveals presence of polycrystalline, perovskite structure corresponding to multilayers of BST/BZT thin films. SEM analysis confirmed the multilayer structure without any interdiffusion across layers. It was also found that the dielectric and ferroelectric properties of the thin films are strongly influenced by the periodic hetero-structures. $(BST/BZT)_n$ films exhibits significantly high tunabilities of ~82% comparable to multilayer thin films grown on different single crystal substrates such as $LaAlO_3$, MgO and $SrTiO_3$. Possible mechanisms explaining the other observed attributes such as lower dielectric loss resulting in higher Figure of Merit (FoM), low leakage current have been explained. The

heterostructure multilayers with compositions at morphotropic phase boundary assisted in realization of enhanced energy storage density efficiency of >80%. The observed properties of such multilayer structured films help in realization of low loss and highly tunable applications.

Acknowledgements

The authors acknowledge the financial support from the Defence Research and Development Organization, Ministry of Defence, New Delhi for carrying out the present work. Also, the authors would like to thank the Director of Defence Metallurgical Research laboratory (DMRL) for permitting publication of this work.

References

1. Q. Li, L. Chen, M. R. Gadinski, S.H. Zhang, G.Z. Zhang, H. Y. Li, A. Haque, L.Q. Chen, T.N. Jakson, Q. Wang, Flexible high-temperature dielectric materials from polymer nanocomposites, Nature, 523, (2015) 576-579. (https://doi.org/10.1038/nature14647).

2. K. Han, Q. Li, C. Chanthad, M.R. Gadinski, G.Z. Zhang, Q. Wang, A Hybrid Material Approach Toward Solution-Processable Dielectrics Exhibiting Enhanced Breakdown Strength and High Energy Density, Adv. Funct. Mater., 25 (2015) 3505-3513. (https://doi.org/10.1002/adfm.201501070).

3. L.B. Kong, S. Li, T.S. Zhang, J.W. Zhai, F.Y.C. Boey, Electrically tunable dielectric materials and strategies to improve their performances, Prog. Mater. Sci., 55, (2010) 840-893. (https://doi.org/10.1016/j.pmatsci.2010.04.004)

4. P. Bao, T. J. Jackson, X. Wang, M. J. Lancaster. 2008, Dielectric characterization of a ferroelectric film in the sub-GHz region, J. Phys. D: Appl. Phys., 41 (2008) 063001. (https://doi.org/10.1088/0022-3727/41/18/185410).

5. M.W. Cole, S.P. Alpay, Performance Enhanced Complex Oxide Thin Films for Temperature Stable Tunable Device Applications: A Materials Design and Process Science Prospective. Ferroelectrics - Material. Croatia : InTech, 2011. (DOI: 10.5772/16406).

6. Z. Xu, D. Yan, D. Xiao, P. Yu, J. Zhu, Dielectric enhancement of $BaSrTi_{1.1}O_3$ / $BaSrTi_{1.05}O_3$ / $BaSrTiO_3$ multilayer thin films prepared by RF magnetron sputtering, Ceram. Int., 39 (2013) 1639-1643. (http://dx.doi.org/10.1016/j.ceramint.2012.08.006).

7. M. W. Cole, E. Ngo, S. Hirsch, and J. D. Demaree, S. Zhong, S. P. Alpay, The fabrication and material properties of compositionally multi-layered $Ba_{1-x}Sr_xTiO_3$ thin films for realization of temperature insensitive tunable phase shifter devices, J. Appl. Phys., 102 (2007) 034104-03411. (DOI: 10.1063/1.2761849).

8. D. Peng, J. Cheng, Z. Meng, Low dielectric dissipation and enhanced tunability of Ba0.6Sr0.4TiO3 thin films by the modified composition and multilayer structure, J. Electroceram., 21 (2008) 668-671. (DOI : 10.1007/s10832-007-9272-6)

9. J. Miao, B. P. Zhang, K. H. Chew, Y. Wang, Improvement of ferroelectric fatigue endurance in multiferroic $(Ba_{0.5}Sr_{0.5})TiO_3$ / $(Bi_{1.05}La_{0.05})FeO_3$ / $(Ba_{0.5}Sr_{0.5})TiO_3$ sandwich structures, Appl. Phys. Lett., 92 (2008) 062902. (DOI: 10.1063/1.2841672).

10. C. Diao, H. Liu, H. Zheng, Z. Yao, J. Iqbal, M. Cao, H. Hao. Enhanced energy storage properties of $BaTiO_3$ thin films by $Ba_{0.4}Sr_{0.6}TiO_3$ layers modulation, J. Alloy. Compd., 765 (2018) 362-368. (https://doi.org/10.1016/j.jallcom.2018.06.199).

11. B. Guigues, J. Guillan, E. Defay, P. Garrec, D. Wolozan, B. Andre, F. Laugier, R. Pantel, X. Gagnard, M. Aıd, $SrTiO_3$/$BaTiO_3$ multilayers thin films for integrated tunable

capacitors applications, J. Eur. Ceram. Soc. , 27 (2007) 3851-3854. (doi:10.1016/j.jeurceramsoc.2007.02.043).

12. A. N. Tarale, M. M. Sutar, D. J. Salunkhe, P. B. Joshi, S. B. Kulkarni, R. C. Pawar, C. S. Lee, D. M. Phase, M. Gupta, R. J. Chaudhary, Dielectric properties of sol–gel synthesized $SrTiO_3/(Ba_{0.7}Sr_{0.3})TiO_3$ and $SrTiO_3/Ba(Zr_{0.3}Ti_{0.7})O_3$ thin film heterostructures J. Mater. Sci: Mater. Electron., 24 (2013) 1308-1318. (DOI 10.1007/s10854-012-0925-0)

13. X. Yan, W. Ren, P. Shi, X. Wu, X. Chen, X. Yao, $Ba_{0.5}Sr_{0.5}TiO_3/Bi_{1.5}Zn_{1.0}Nb_{1.5}TiO_7$ multilayer thin films prepared by sol–gel method, Appl. Surf. Sci., 255 (2008) 2129-2132. (doi:10.1016/j.apsusc.2008.07.045).

14. X.Y. Chen, Z.P. Xu, D.X. Yan, Y.S. Fan, J.G. Zhu, P. Yu, Great enhancement of polarization in the $(Ba_{0.67}Sr_{0.33}TiO_3/LaNiO_3)n$ multilayer thin films, J. Alloys. Compd., 695 (2017) 1913-1917. (https://doi.org/10.1016/j.jallcom.2016.11.025).

15. J. Miao, H. Y. Tian, X. Y. Zhou, K. H. Pang, Y. Wang, Microstructure and dielectric relaxor properties for $Ba_{0.5}Sr_{0.5}TiO_3/La_{0.67}Sr_{0.33}MnO_3$ heterostructure, J. Appl. Phys., 101 (2007) 084101. (DOI: 10.1063/1.2721393).

16. J. Liao, X. Wei, Z. Xu, X. Wei, P. Wang, The structure and dielectric properties of a novel kind of doped $Ba_{0.6}Sr_{0.4}TiO_3$ film, Mater. Chem. Phys.,135 (2012) 1030-1035. (http://dx.doi.org/10.1016/j.matchemphys.2012.06.009).

17. S. X. Wang, M. S. Guo, X. H. Sun, T. Liu, M. Y. Li, X. Z. Zhao, Tunable, low loss $Bi_{1.5}Zn_{1.0}Nb_{1.5}O_7/Ba_{0.6}Sr_{0.4}TiO_3/Bi_{1.5}Zn_{1.0}Nb_{1.5}O_7$ sandwich films, Appl. Phys. Lett., 89 (2006) 212907. (DOI: 10.1063/1.2393093).

18. S. Z. Wang, J. X. Liao, T. T. Feng, Y. M. Hu, H. Y. Yang, M. Q. Wu, Structures and dielectric properties of multilayer BST/ST/BST and ST/BST/ST sandwich structures, Integr. Ferroelectr., 170 (2016) 120-129. (https://doi.org/10.1080/10584587.2016.1170513).

19. J. Singh, S.B. Krupanidhi, Multilayer $Bi_{1.5}Zn_{1.0}Nb_{1.5}O_7/Ba_{0.6}Sr_{0.4}TiO_3/Bi_{1.5}Zn_{1.0}Nb_{1.5}O_7$ thin films for tunable microwave applications, App. Surf. Sci., 257 (2011) 2214-2217. (doi:10.1016/j.apsusc.2010.09.076).

20. Y. Bian, J. Zhai, Low dielectric loss $Ba_{0.6}Sr_{0.4}TiO_3/MgTiO_3$ composite thin films prepared by a sol–gel process, J. Phys. Chem. Solids, 75 (2014) 759-764. (http://dx.doi.org/10.1016/j.jpcs.2014.02.002)

21. N. Zhao, L. Wan, L. Cao, D. Yu, S. Yu, R. Sun, Dielectric enhancement of $BaTiO_3/BaSrTiO_3/SrTiO_3$ multilayer thin films deposited on $Pt/Ti/SiO_2/Si$ substrates by sol–gel method, Mater. Lett., Vol. 65 (2011) 3574-3576. (doi:10.1016/j.matlet.2011.08.004).

22. D. Bao, Multilayered dielectric/ferroelectric thin films and superlattices, Curr. Opin. Solid St. M., 12 (2008) 55–61. (doi:10.1016/j.cossms.2009.01.006).

23. F. Yan, Y. Wang, H. L. W. Chan, C. L. Choy, Ferroelectric properties of $(Ba_{0.5}Sr_{0.5})TiO_3$ / $Pb(Zr_{0.52}Ti_{0.48})O_3$ / $(Ba_{0.5}Sr_{0.5})TiO_3$ thin films with platinum electrodes, Appl. Phys. Lett., 82 (2003) 4325. (DOI: 10.1063/1.1583137).

24. Y. Wang, J.Cui, Q. Yuan, Y. Niu, Y. Bai, H. Wang, Significantly Enhanced Breakdown Strength and Energy Density in Sandwich-Structured Barium Titanate/Poly(vinylidene fluoride) Nanocomposite, Adv. Mater., 27 (2015) 42. (DOI :https://doi.org/10.1002/adma.201503186).

25. M.L.V. Mahesh, V.V. Bhanu Prasad, A.R. James, Enhanced dielectric and ferroelectric properties of lead-free $Ba(Zr_{0.15}Ti_{0.85})O_3$ ceramics compacted by cold isostatic pressing, J. Alloys Comp., 611 (2014) 43-49. (http://dx.doi.org/10.1016/j.jallcom.2014.05.098).

26. M.L.V. Mahesh, V.V. Bhanuprasad, A.R. James. Enhanced Piezoelectric Properties and Tunability of Lead-Free Ceramics Prepared by High-Energy Ball Milling, J. Electron. Mater., 42 (2013) 3547. (DOI: 10.1007/s11664-013-2812-8).

27. M. L. V. Mahesh, A. R. James, Dependence of $Ba(Zr_{0.15}Ti_{0.85})O_3$ films growth on substrate temperature and oxygen gas pressure prepared by pulsed laser deposition, J. Nanopart. Res., 17 (2015) 482-488. (DOI 10.1007/s11051-015-3292-y).

28. M. L. V. Mahesh, A.R. James, V.V. Bhanu Prasad. In-situ post deposition annealing of lead-free ferroelectric thin films in oxygen rich atmosphere, J Mater Sci: Mater Electron, 26 (2015) 4930-4935. (DOI 10.1007/s10854-015-3004-5).

29. Y.L. Li, S.Y. Hu, D. Tenne, A. Soukiassian, D.G. Schlom, L.Q. Chen, X.X. Xi, K.J. Choi, C.B. Eom, A. Saxena, T. Lookman, Q.X. Jia, Interfacial coherency and ferroelectricity of $BaTiO_3$/$SrTiO_3$ superlattice films, Appl. Phys. Lett., 91 (2007) 112914. (https://doi.org/10.1063/1.2823608).

30. H. Christen, E.D. Specht, S.S. Silliman, K.S. Harshavardhan, Ferroelectric and antiferroelectric coupling in superlattices of paraelectric perovskites at room temperature, Phys. Rev. B, 68 (2003) 020101(R). (https://doi.org/10.1103/PhysRevB.68.020101).

31. Q. Zhang, J. Zhai L. B. Kong, J. Adv. Dielect., 2 (2012), 123002.

32. W. F. Qin, J. Zhu, J. Xiong, J. L. Tang, W. J. Jie, Y. Zhang, Y. R. Li, Dielectric characteristics of BST/BZT/BST multilayer, Surf. Rev. Lett., 15 (2008), 195-200. (https://doi.org/10.1142/S0218625X08011238).

33. M. Liu, C. Ma, J. Liu, G. Collins, C. Chen, F. Xiang, H. Wang, J. He, J. Jiang, E. I. Meletia, A. Bhalla, Microwave Dielectric Properties of Mn-doped $(Ba,Sr)TiO_3$//$Ba(Zr,Ti)O_3$ Multilayered Thin Films: Optimization of Designed Structure, Integ. Ferro., 150 (2014), 116-122. (DOI: 10.1080/10584587.2014.874838).

34. N.Y. Chan, G.Y. Gao, Y. Wang, H.L.W. Chan, Preparation and characterizations of $Ba(Zr,Ti)O_3$/$(Ba,Sr)TiO_3$ heterostructures grown on $(LaAlO_3)_{0.3}(Sr_2AlTaO_6)_{0.35}$

single crystal substrates by pulsed laser deposition, Thin Solid Films , 518 (2010),e82-e84. (doi:10.1016/j.tsf.2010.03.088).

35. O. Nakagawara, T. Shimuta, T. Makino, S. Arai, Epitaxial growth and dielectric properties of (111) oriented $BaTiO_3/SrTiO_3$ superlattices by pulsed-laser deposition, Appl. Phys.Lett., 77 (2000) 3257. (S0003-6951~00!00646-X).

36. J. Wang, F. Guan, L. Cui, J. Pan, Q. Wang, L. Zhu, Achieving High Electric Energy Storage in a Polymer Nanocomposite at Low Filling Ratios using a Highly Polarizable Phthalocyanine Interphase, J. Polym. Sci., Part B: Polym. Phys., 52 (2014) 1669-1680. (DOI: 10.1002/polb.23554).

37. Y. Gao, H. Liu, Z. Yao, H. Hao, Z. Yu, M. Cao, Effect of layered structure on dielectric properties and energy storage density in $xBa_{0.7}Sr_{0.3}TiO_3$-$SrTiO_3$ multilayer ceramics, Ceram. Int., 43 (2017) 8418-8423. (https://doi.org/10.1016/j.ceramint.2017.03.190).

38. K.M. Johnson, Variation of dielectric constant with voltage in ferroelectrics and its application to parametric devices, J. Appl. Phys., 33 (1962) 2826. (https://doi.org/10.1063/1.1702558)

39. A.F. Devonshire, Theory of barium titanate, Philos. Mag., 40 (1949) 1040-1063. (https://doi.org/10.1080/14786444908561372).

40. S. Yu, C. Zhang, M. Wu, H. Dong, L. Li, Ultra-high energy density thin-film capacitors with high power density using $BaSn_{0.15}Ti_{0.85}O_3/Ba_{0.6}Sr_{0.4}TiO_3$ heterostructure thin films, J. Power Sources., 412 (2019) 648-654. (https://doi.org/10.1016/j.jpowsour.2018.12.012).

41. Z. Sun, L. Wang, M. Liu, C. Ma, Z. Liang, Q. Fan, L. Lu, X. Lou, H. Wang, C. Jia. 2018, Interface-Thickness Optimization of Lead-Free Oxide Multilayer Capacitors for High-Performance Energy Storage, J. Mater. Chem. A, 6 (2018) 1858-1864. (DOI 10.1039/C7TA10271B).

Figures

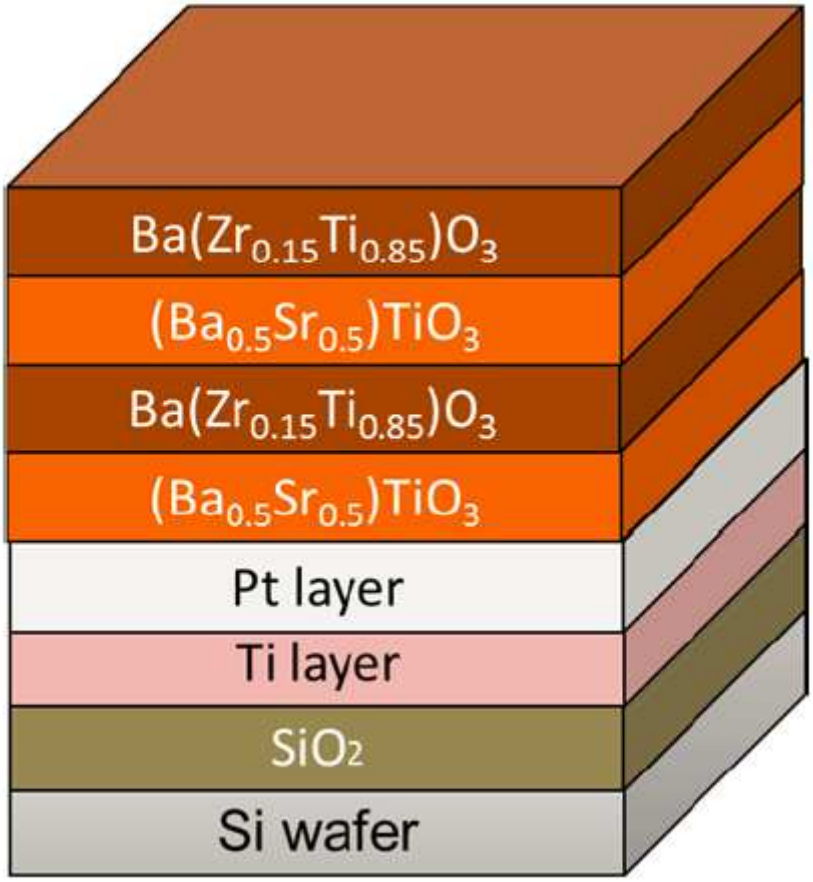

Figure 1

Schematic of multilayer structure consisting of bilayer stack of (Ba0.50Sr0.50)TiO3 and Ba(Zr0.15Ti0.85)O3 thin films

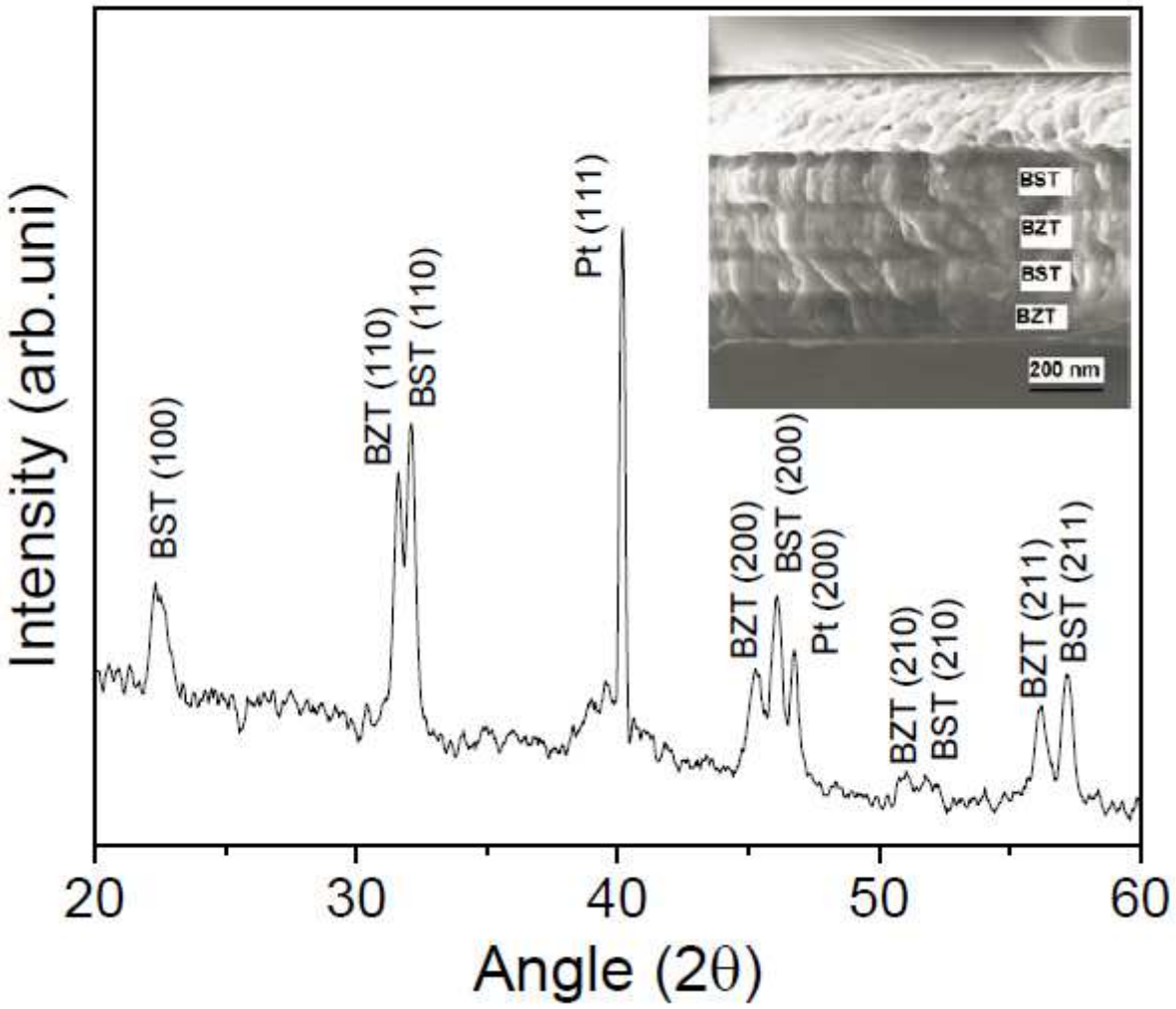

Figure 2

X-ray diffractograms of (Ba0.50Sr0.50)TiO3 and Ba(Zr0.15Ti0.85)O3 multilayer thin films (inset) Cross section SEM images depicting multilayer structure.

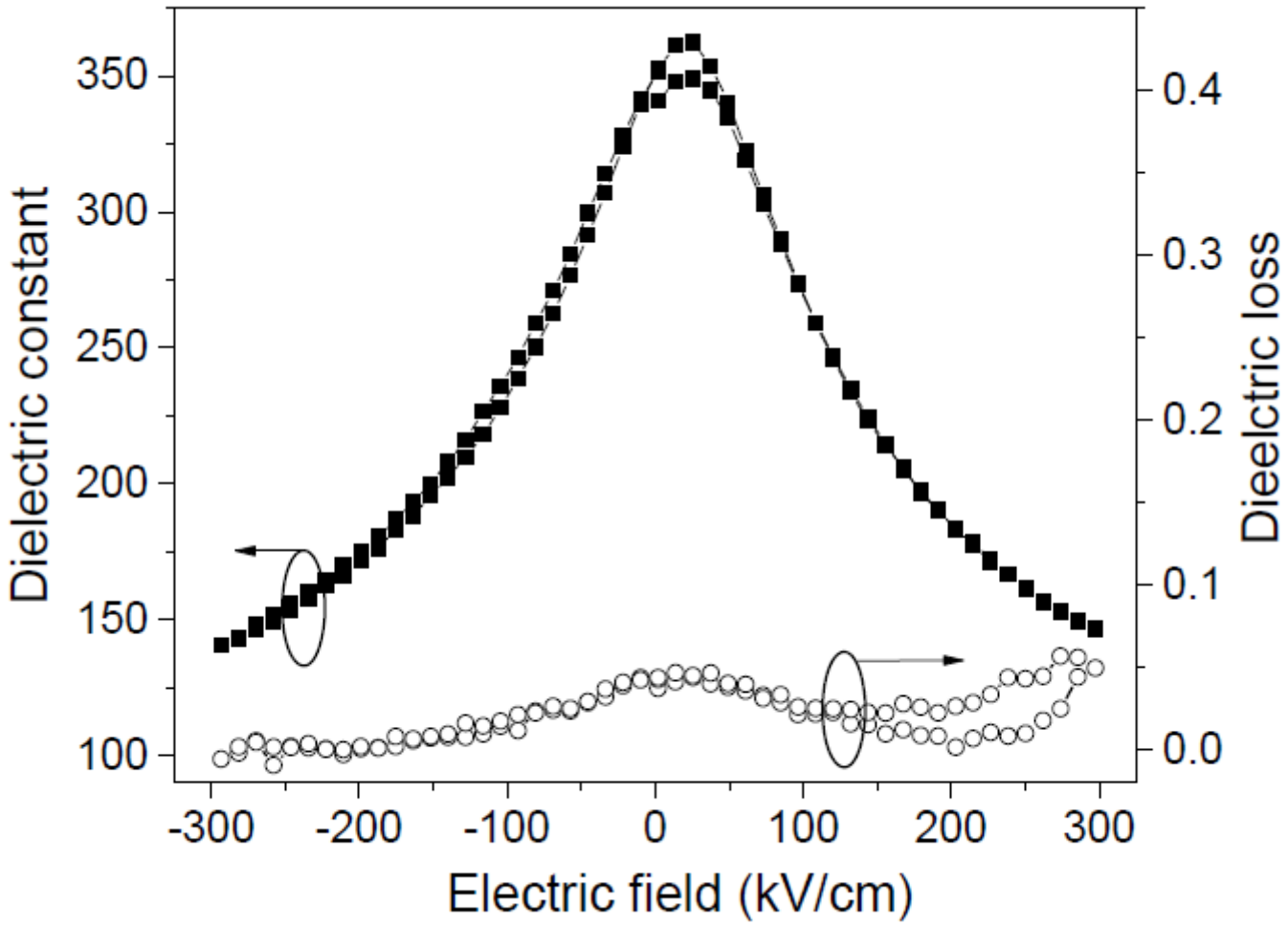

Figure 3

Electric field dependence of dielectric permittivity and dielectric loss corresponding to bilayers of (Ba0.50Sr0.50)TiO3 and Ba(Zr0.15Ti0.85)O3 multilayer thin films at room temperature.

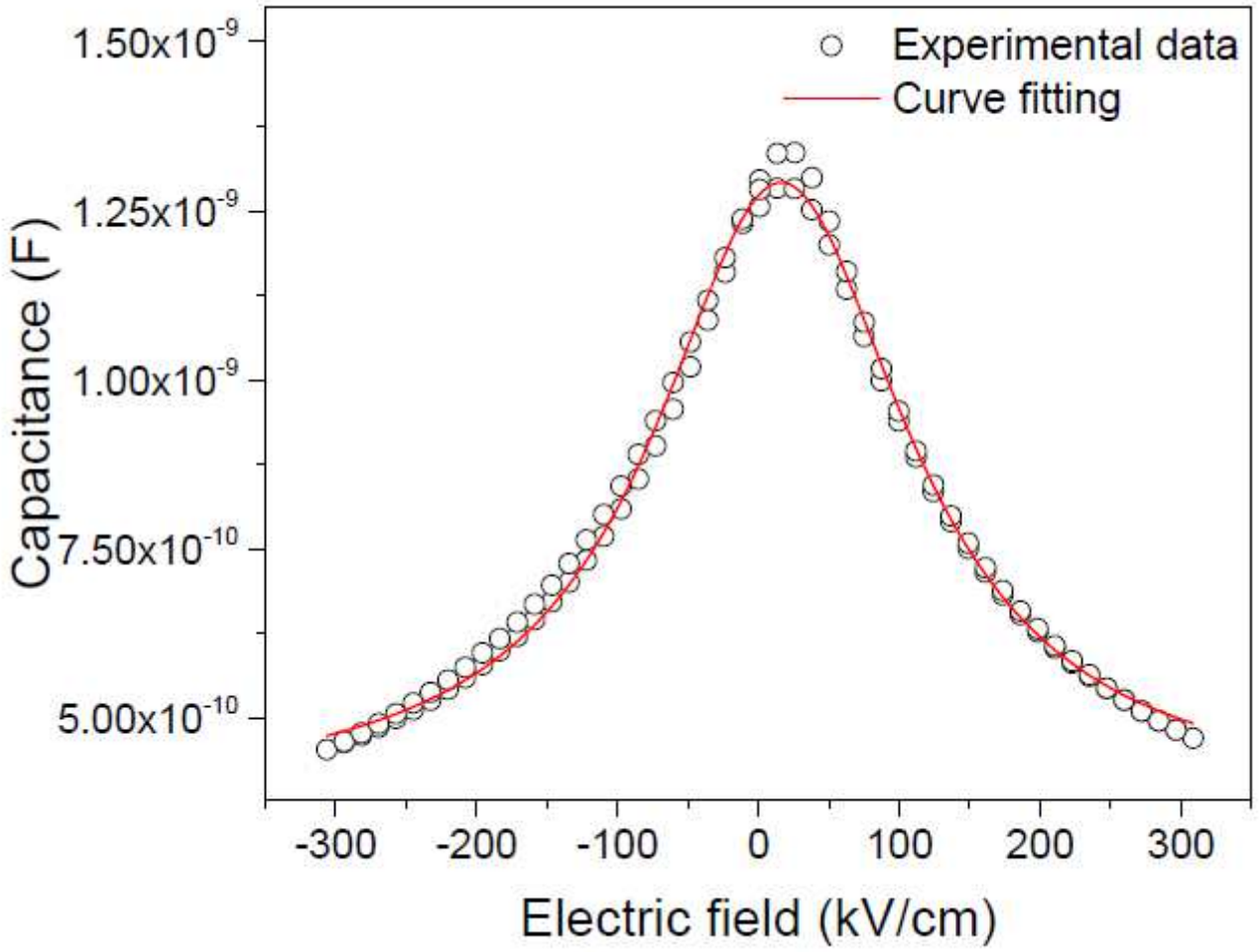

Figure 4

Capacitance as a function of electric field corresponding to bilayers of (Ba0.50Sr0.50)TiO3 and Ba(Zr0.15Ti0.85)O3 multilayer thin films.

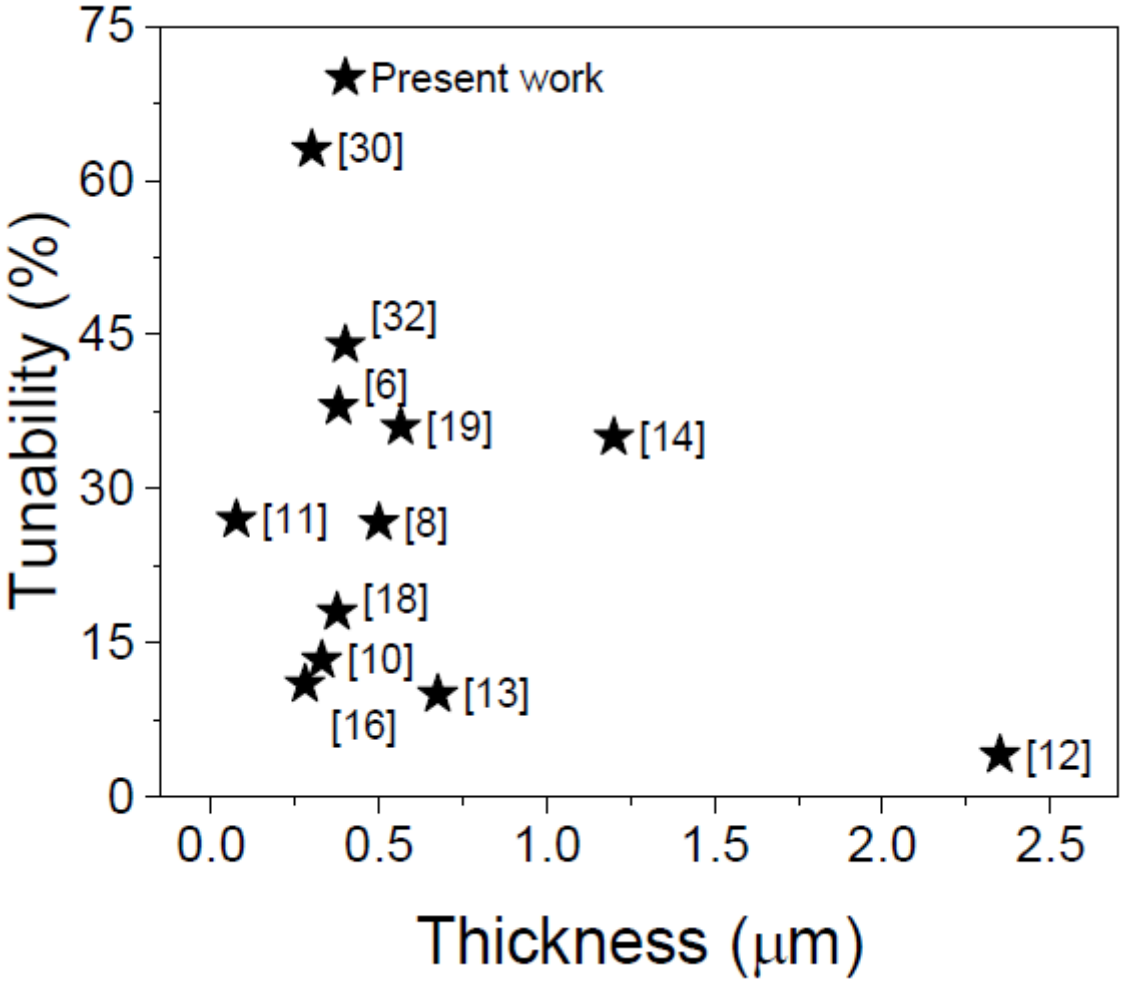

Figure 5

Reported tunabilities of different lead-free multilayer thin films vs total thickness of the grown multilayers using different processing techniques and substrates.

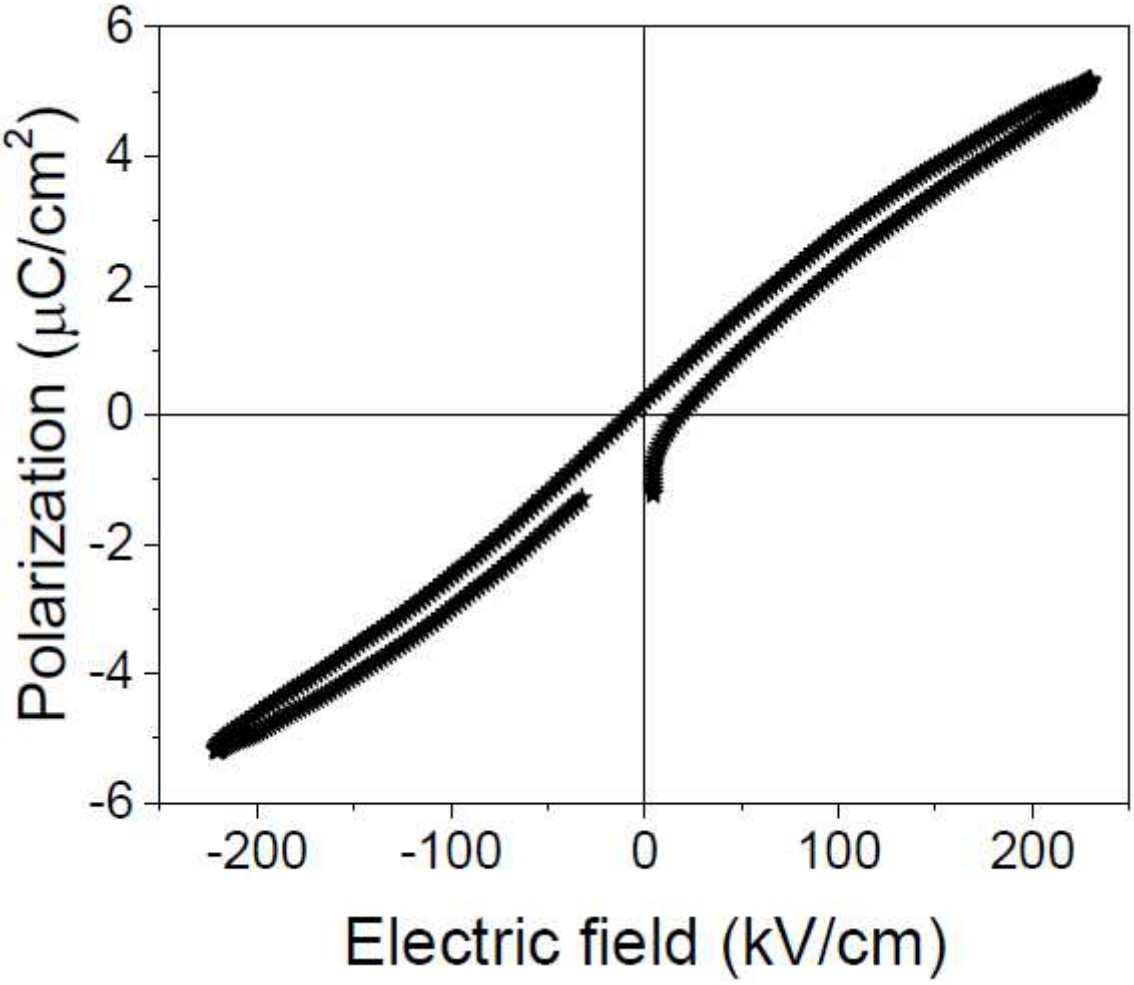

Figure 6

Evolution of ferroelectric hysteresis loops with respect to the electric field corresponding to lead-free multilayer thin films

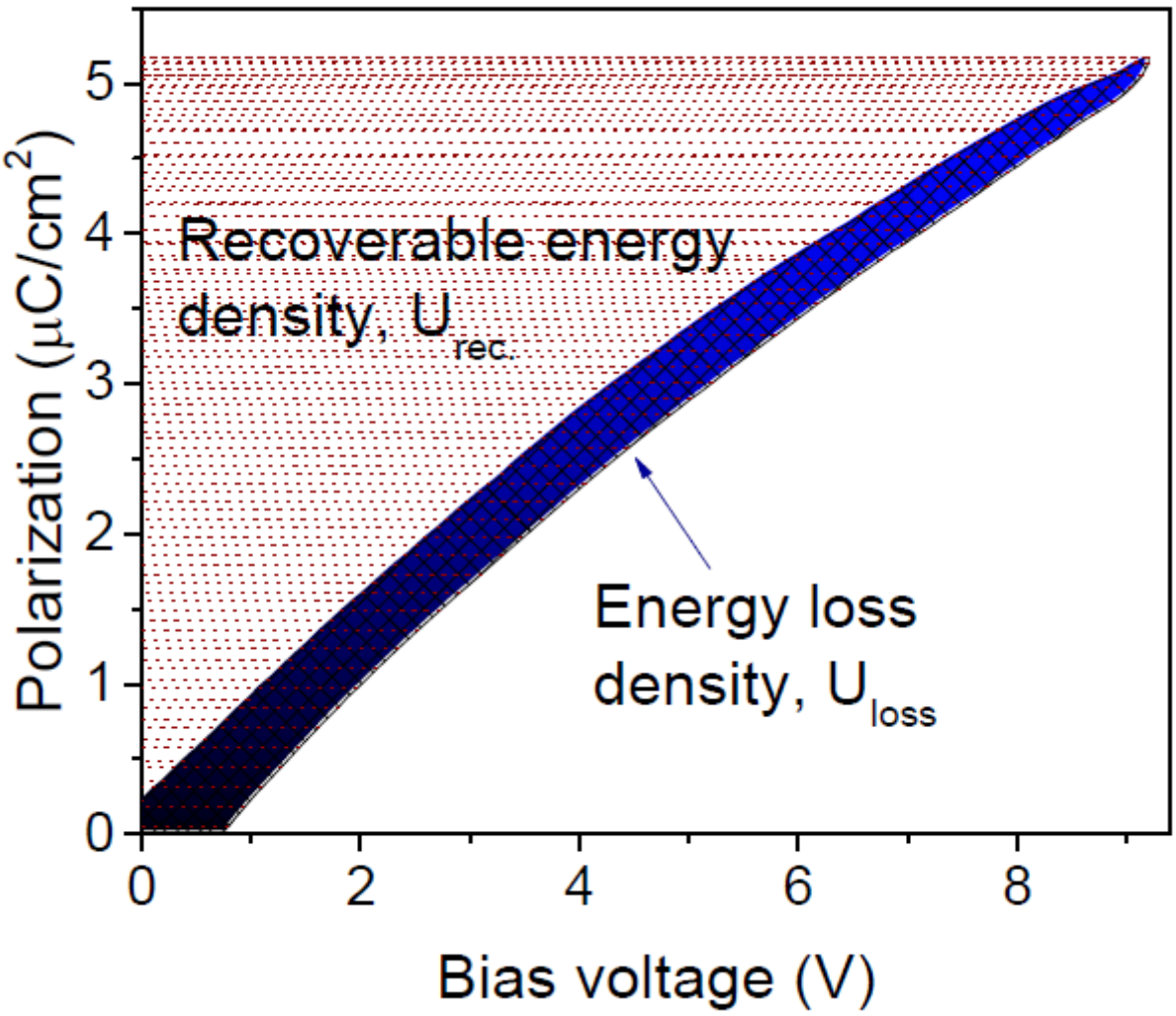

Figure 7

Polarization vs bias voltage loops highlighting the recoverable energy density, Urec and energy loss, Uloss

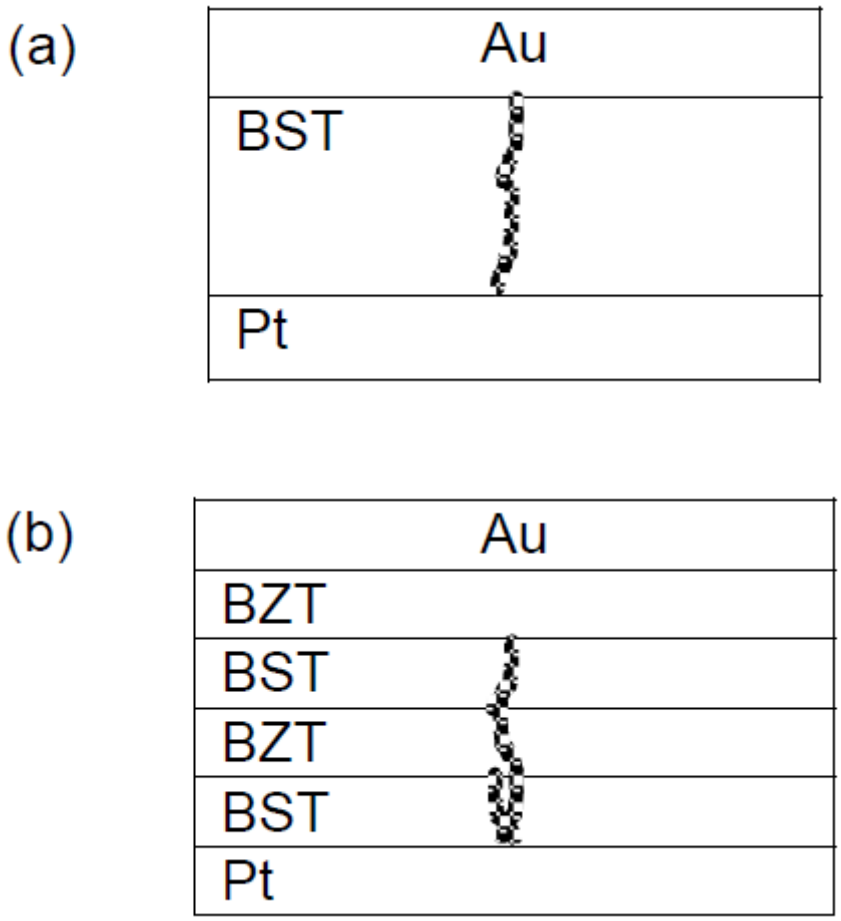

Figure 8

Schematic illustrating propagation of leakage current conducting path in (a) (Ba0.50Sr0.50)TiO3 thin film and (b) Multilayer thin films of (Ba0.50Sr0.50)TiO3 and Ba(Zr0.15Ti0.85)O3 bilayers.